Neutron powder diffraction investigation in ammonium iron(III) bis (hydrogenphosphate)

Neutron powder diffraction investigation in ammonium iron(III) bis (hydrogenphosphate)

B. F. Alfonso[1], C. Piqué[1], C. Trobajo[2], J. R. García[2], E. Kampert[3], I. Mirebeau[4], N. Rey[4], J. Rodríguez Fernández[5], M. T. Fernández-Díaz[6], J. A. Blanco[1]

[1]Departamento de Física, Facultad de Ciencias, Universidad de Oviedo, E–33007 Oviedo, Spain
[2]Departamento de Química Orgánica e Inorgánica, Facultad de Química, Universidad de Oviedo, E–33006 Oviedo, Spain
[3] Helmholtz-Zentrum Dresden-Rossendorf, Dresden High Magnetic Field Laboratory, D-01314 Dresden, Germany
[4]Laboratoire Léon Brillouin. (CEA-CNRS). CEN-Saclay, F-91191. Gif-sur-Yvette. Cedex, France
[5]CITIMAC, Facultad de Ciencias, Universidad de Cantabria, E–39005 Santander, Spain
[6]Institute Laue-Langevin, B. P. 156X, F–38042, Grenoble, France

E-mail: jabr@uniovi.es

Abstract. The deuterated form of ammonium iron(III) bis (hydrogenphosphate), $ND_4Fe(DPO_4)_2$, was investigated in detail from neutron powder diffraction data with a wavelength $\lambda = 4.724$ Å. The material undergoes two successive magnetic phase transitions which are associated with the Fe^{3+} magnetic moments. One at $T_C = 17.82 \pm 0.05$ K is attributed to the ferrimagnetic order with the magnetic moments, $\mu_{FI} = 4.19 \pm 0.02\ \mu_B$ at 4 K, lying on the crystallographic plane *ac*. The other transition is found to be at $T_t = 3.52 \pm 0.05$ K due to an antiferromagnetic arrangement, with an equal moment antiphase structure that is characterized by a long–period propagation vector close to $\vec{k}_{AF} \approx (1/16, 0, 1/16)$ and a magnetic moment for the Fe^{3+} ions of $\mu_{AF} = 4.41 \pm 0.03\ \mu_B$ at 1.5 K. The low symmetry of its triclinic crystal structure and the complex pattern of competing superexchange pathways seem to be responsible for the existence of this double magnetic phase transition.

1. Introduction

During the last century a considerable attention has been paid to porous crystalline materials, known as open metal framework systems, which are currently a hot topic of research. Porous materials such as zeolites have an important industrial and environmental applications ranging to catalysis, ion-exchange, sensing, separation and removal of contaminants and more [1, 2, 3]. In particular, iron phosphates are attractive because of their striking magnetic properties [4, 5, 6]. Recently we have focused our interest on $ND_4Fe(DPO_4)_2$ because it appears to behave magnetically in a complex manner. In previous works of $ND_4Fe(DPO_4)_2$ we have investigated the crystal and magnetic structures from neutron powder diffraction [7, 8] together with the physical properties [9]. The magnetic and specific heat measurements revealed the existence of two magnetic phases at low temperatures. The magnetic moments of the Fe^{3+} ions order ferrimagnetically below $T_C = 17.82 \pm 0.05$ K and they undergo a magnetic phase transition below

$T_t = 3.52 \pm 0.05$ K for adopting an antiferromagnetic arrangement, as was clearly evidenced from the temperature dependence of the magnetization under low applied magnetic field.

The intermediate and low–temperature magnetic structures were investigated from neutron powder diffraction on D2B (λ = 1.594 Å) and D1B (λ = 2.524 Å). The patterns collected between T_t and T_C indicate the existence of a ferrimagnetic (FI) arrangement involving the three Fe magnetic moments within the crystallographic cell. While the powder patterns below T_t show only some few new additional magnetic reflections, which could be indexed with a propagation vector close to a long–period commensurate vector. The best refinement (R_{mag} = 10.9 %) corresponds to an antiphase magnetic structure which is formed from the same magnetic unit of the FI ordering observed at higher temperatures. The determination of this magnetic structure is not straightforward. On the one hand, the number of the magnetic Bragg reflections is not large and they have moderate intensity, overlapping in some cases with the nuclear peaks. And, on the other, the absence of the Bragg reflections corresponding to the principal and the high-order harmonics (perhaps because they could be found at very low Bragg angles inside the central neutron beam on D1B and D2B diffractometers) makes very difficult the determination of the propagation vector. In order to overcome these problems, we have performed further neutron experiments with a neutron–wavelength larger than $\lambda = 2.524$ Å ($\lambda = 4.724$ Å), with the aim to obtain information on large magnetic interplanar distances, which could allow us to detect the existence of the principal and the higher-order harmonics of the propagation vector.

2. Experimental details

The neutron powder diffraction experiments were performed on the G61 ($\lambda = 4.724$ and 4.755 Å) diffractometer at the Laboratoire Léon Brillouin (LLB), Paris (France). Data were collected at several selected temperatures: 30, 4 and 1.5 K. Rietveld refinements of the crystal and magnetic structures were carried out using the FULLPROF program [10].

3. Results

The nuclear pattern collected at 30 K on G61 was fitted using a triclinic $P\bar{1}$ space group (see Fig. 1). The atomic model reported from our neutron powder experiments on D2B diffractometer [7, 8] was used as starting atomic model for the G61 experiment. Within the experimental uncertainties the results are the same: the primitive unit cell of $ND_4Fe(DPO_4)_2$ contains three Fe^{3+} ions on two different crystallographic sites with different local symmetry, one Fe1 located at the spatial inversion center and two Fe2 ions, Fe2(1) and Fe2(2), located on a crystalline site with only the identity symmetry.

As expected, the pattern collected at 4 K on G61 does not show any extra peaks different from those found at 30 K. All the magnetics peaks can be indexed with a propagation vector $\vec{k} = (0, 0, 0)$ referring to the 30 K crystallographic unit cell, indicating that the magnetic and nuclear unit cells are the same (Fig. 1). The directions of the magnetic moments of the two Fe1 and Fe2 sublattices are antiparallel lying on the *ac*-plane of the crystal structure. Therefore, the magnetic moments have a FI ordering with an arrangement ↑↓↑ (see Fig. 2 (a)), the Fe2 magnetic moments being ↑, while the Fe1 one is ↓. Table 1 shows the final refinement of components for the magnetic moments, in the ferrimagnetic phase, along the crystallographic directions of the primitive unit cell (a, b, c) obtained from G61 and those reported on D1B. The agreement between the values of the magnetic moment obtained in the two experiments is quite good, it allows us to confirm the FI character of the intermediate magnetic structure obtained from the experiment carried out on D2B and D1B.

The neutron powder diffraction experiment at 1.5 K (Fig. 1) was used to determine the low–temperature magnetic structure. The magnetic pattern shows additional satellite reflections, characteristic of an antiferromagnetic ordering. Their position appears to be incommensurate with regard to the nuclear lines. The determination of the propagation vector has been done

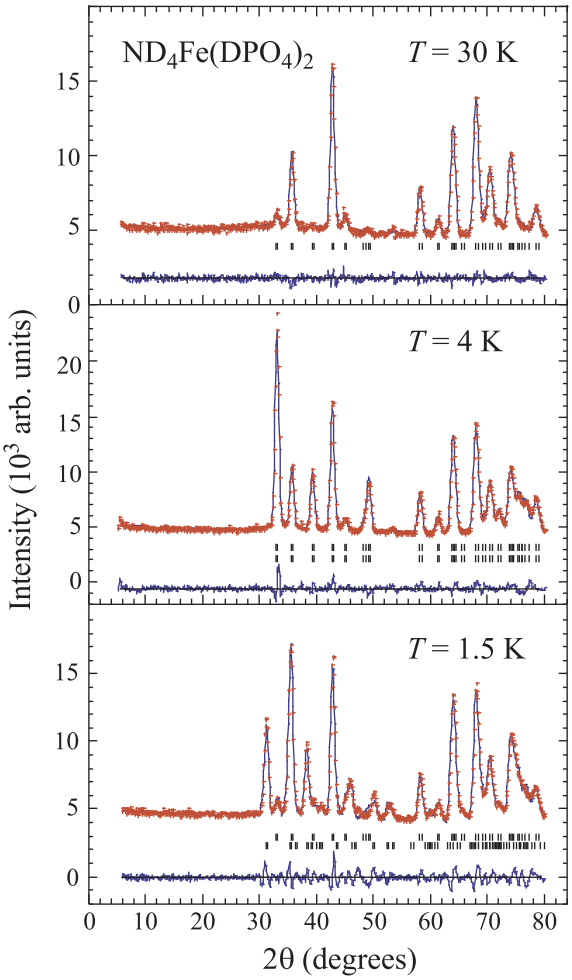

Figure 1. (Color online) Neutron powder diffraction refinement for $ND_4Fe(DPO_4)_2$. Observed (points) and calculated (solid line) collected on G61 at 30, 4 and 1.5 K. Bragg reflection positions are represented by vertical bars. The first (second) raw of Bragg diffraction reflections corresponds to the nuclear (magnetic) peaks. The observed-calculated difference is depicted at the bottom of each pattern.

graphically by following the method described by Chevalier et al. [11]. First, the basis vectors $\vec{a}^*$, $\vec{b}^*$, $\vec{c}^*$ of the reciprocal space are calculated from the cell parameters of the direct space. The reciprocal space of the crystal structure of $ND_4Fe(DPO_4)_2$ and the first Brillouin zone associated

Table 1. Components of the iron magnetic moments in $ND_4Fe(DPO_4)_2$ at 4 K (a) on G61 and (b) on D1B, with the following constraints: $\vec{\mu}_{Fe1} = -\vec{\mu}_{Fe2}$ and $\vec{\mu}_{Fe2(1)} = \vec{\mu}_{Fe2(2)}$.

	$\mu_{Fe_{1a}}$ (μ_B)	$\mu_{Fe_{1b}}$ (μ_B)	$\mu_{Fe_{1c}}$ (μ_B)	$\lvert\vec{\mu}\rvert$ (μ_B)	R_{mag} (%)	Ref.
(a)	-3.56(9)	0	-5.81(7)	4.19(2)	3.8	This work
(b)	-3.77(15)	0	-5.84(13)	4.20(12)	5.3	[8]

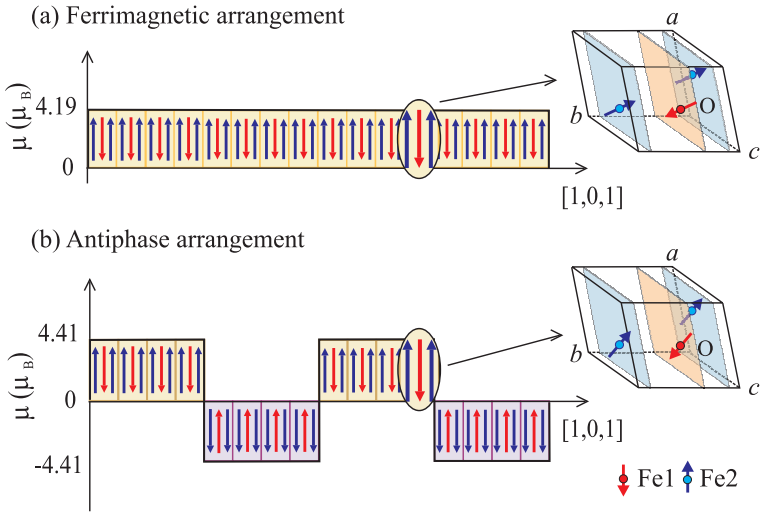

Figure 2. (Color online) Schematic representation of (a) the ferrimagnetic structure with a $\mu = 4.19(2)$ μ_B at 4 K, and (b) the antiphase magnetic structure at 1.5 K for $ND_4Fe(DPO_4)_2$ along the direction of propagation vector $\vec{k}_{AF} = (\tau, 0, \tau)$ with $\tau \equiv 1/16$ and $\mu = 4.41(3)$ μ_B. In all the cases the magnetic moments are lying in the ac–plane (see text).

with the Bravais lattice are drawn in Fig. 3. Using the Bragg relation, Eq. (1), we calculate the modulus of the scattering vector $\vec{Q}$ for the Bragg's angles corresponding to the magnetic reflections (found at low angles, see Fig. 1). We plot spheres of radius $|\vec{Q}|$ centered at the origin (000) of the reciprocal space.

$$| \vec{Q} | = 4\pi sin\theta/\lambda \tag{1}$$

$$| \vec{Q} | = | \vec{K} \pm \vec{k} | \tag{2}$$

Due to the Bragg condition expressed by the Eq. (2), where $\vec{K}$ is a reciprocal lattice vector and $\vec{k}$ is the magnetic propagation vector, it is necessary to find the intersection of these spheres of radius $|\vec{Q}|$ with the small sphere of radius $|\vec{k}|$, centered at each point in the reciprocal space, in such a way that the ends of the diameter at the point of intersection cut the spheres of radius $|\vec{Q}|$ in the same direction for all the points of the reciprocal space. Then, the radius of the small sphere give us the magnetic propagation vector: $\vec{k} = (0.06, 0, 0.06)$ rlus (reciprocal lattice units). This propagation vector has been successfully used for indexing the magnetic neutron powder diffraction pattern collected at 1.5 K. The nearest long-period commensurate propagation vector is close to $\vec{k}_{AF} = (\tau, 0, \tau)$ with $\tau \equiv 1/16$ (the same propagation vector as that determined on D1B). The magnetic periodicity is repeated after 16 crystallographic unit cells along the a and c directions. The best fit to the experimental data corresponds to a longitudinal–amplitude modulated structure (sine–wave type) with the magnetic moments lying in the ac–plane, the maximum amplitude of the sine–wave modulated moment being 5.61(3) μ_B. The reliability factor for the Rietveld refinement obtained from experiments on G61 is $R_{mag} = 4.4$ %, which is better than that from D1B, $R_{mag} = 10.9$ %. Table 2 shows the position and intensity of the calculated and observed magnetic Bragg reflections that appear for angles 2θ less than 53^o. Due to the fact that Fe^{3+} ion is a Kramers ion, this means that the magnetic moment over each site can not be zero at zero temperature, as it would be expected for a sine-wave magnetic structure. This circumstance implies that the magnetic arrangement found at 1.5 K for $ND_4Fe(DPO_4)_2$

Table 2. Positions and intensity of the magnetic Bragg reflections in $ND_4Fe(DPO4)_2$ at 1.5 K (see Fig. 1) [calc: calculated, obs: observed, and $(hkl)^{\pm\tau} \equiv (hkl)^{\pm} = (hkl) \pm (\tau, 0, \tau)$ with $\tau \equiv 1/16$ in rlus]. Both intensities are corrected by a Lorentz factor of $\sin 2\theta \sin\theta$. The intensities are calculated with a Fe sine–wave amplitude modulated moment having a maximum amplitude of 5.61(3) μ_B (see text).

2θ (°)	(hkl)	I_{calc} (arb. units)	I_{obs} (arb. units)
31.240	$(010)^-$	542.3	563.5
35.373	$(010)^+$	668.9	669.0
35.471	$(\bar{1}01)^-$	144.8	143.9
38.200	$(\bar{1}\bar{1}1)^+$	538.1	546.7
40.865	$(\bar{1}\bar{1}1)^-$	126.0	116.6
43.398	$(001)^-$	150.4	143.1
46.278	$(1\bar{1}0)^-$	233.6	239.8
52.340	$(1\bar{1}0)^+$	275.9	296.0

must evolve at low temperatures towards an equal–moment magnetic structure or antiphase ordering, where the magnetic moments over an Fe site are described by the squaring–up [12]:

$$\vec{\mu}_{lj} = \frac{4}{\pi} \times \sum_{p=0}^{\infty} \frac{\mu_j}{2p+1} sin((2p+1)\vec{k}\vec{R}_{lj}) \tag{3}$$

where $\vec{\mu}_{lj}$ is the magnetic moment of the Fe^{3+} ions located at the vector position $\vec{R}_{lj}$ (with the index j runs for Fe1 and Fe2, l is a composite index for a lattice translation, $\vec{R} = l_1\vec{a} + l_2\vec{b} + l_3\vec{c}$, where l_i are all integers), $2p+1$ (with $p = 0, 1, 2, ...$) are the 1^{st}, 3^{rd}, 5^{th}, ... order harmonics and $\vec{\mu}_j$ is the equal–magnetic moment value of the iron ions. Similarly to the ferrimagnetic magnetic structure observed above $T_t = 3.52 \pm 0.05$ K, we have found that the best solution for the antiphase ordering corresponds to the case with the same constraints of the magnetic moments, *ie,* $\vec{\mu}_{Fe1} = -\vec{\mu}_{Fe2}$ and $\vec{\mu}_{Fe2(1)} = \vec{\mu}_{Fe2(2)}$.

It is worth noting that the principal harmonic $(000)^{\pm\tau}$ and the higher-order harmonics $(000)^{\pm n\tau}$ were not observed. To start with the first harmonics, as can see in Fig. 3, the sphere whose radius is the modulus of the propagation vector is inside the sphere corresponding to the lower angle measured on the three diffraction experiments: D2B ($\lambda = 1.594$ Å, $2\theta_{min} = 8.5^o$), D1B ($\lambda = 2.524$ Å, $2\theta_{min} = 6.2^o$) and G61 ($\lambda = 4.724$ Å, $2\theta_{min} = 5.5^o$). Then, in our case the principal reflection $(000)^{\pm\tau}$ is masked by the central beam. Other high–order harmonics such as $(000)^{\pm 3\tau}$ and $(000)^{\pm 5\tau}$ are expected to be found in the Bragg–angular range 2θ $(14°, 26°)$, but they are not observed, probably because these high–order harmonics are difficult to be

Table 3. Components of the iron magnetic moment in $ND_4Fe(DPO_4)_2$ (a) on G61 at 1.5 K and (b) on D1B at 1.89 K, with the following constraints: $\vec{\mu}_{Fe1} = -\vec{\mu}_{Fe2}$ and $\vec{\mu}_{Fe2(1)} = \vec{\mu}_{Fe2(2)}$.

	$\mu_{Fe_{1a}}$ (μ_B)	$\mu_{Fe_{1b}}$ (μ_B)	$\mu_{Fe_{1c}}$ (μ_B)	$\lvert\vec{\mu}\rvert$ (μ_B)	R_{mag} (%)	Ref.
(a)	-5.81(12)	0	-6.15(9)	4.41(3)	4.4	This work
(b)	-6.13(30)	0	-6.98(30)	4.78(8)	10.9	[8]

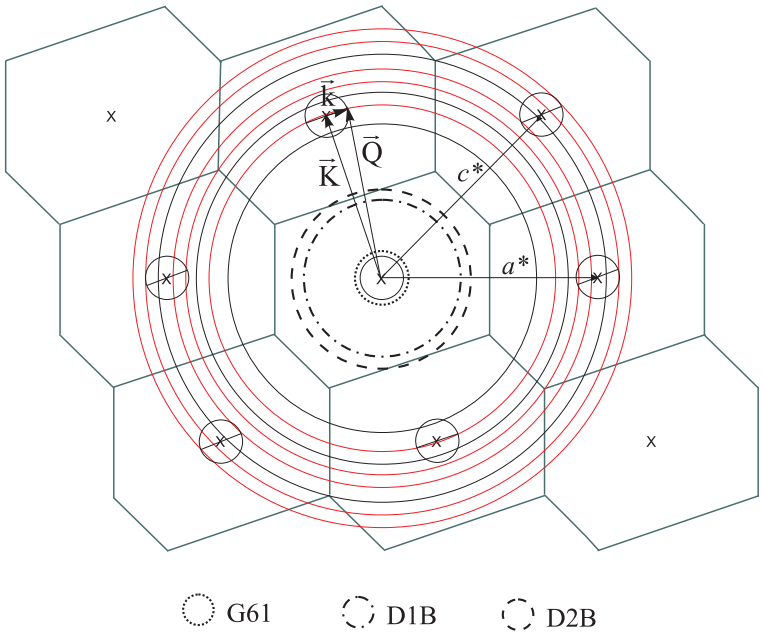

Figure 3. (Color online) Graphical determination of the propagation vector associated with the magnetic structure for $ND_4Fe(DPO_4)_2$ at 1.5 K (see text). The spheres corresponding to the lower angle measured on the three diffractometers: D2B (dashed lines), D1B (dot-dashed lines) and G61 (dots).

seen from a powder experiment, and they are often developed at very low temperatures with regard the magnetic transition temperature [13]. Apart from that, the direction of the magnetic moment in the ac–plane is quite close to direction of the propagation vector. In order to elucidate these different possibilities, we need to perform further experiments with a wavelength larger than $\lambda = 4.724$ Å. Taking into account all these points, the equal–moment magnetic structure has then a magnetic moment of $|\vec{\mu}_j| = 4.41(3)\ \mu_B$, as a result from Eq. (3), where the maximum amplitude associated with the sinus–wave, $5.61(3)\ \mu_B$, can be equalized to the expression $\frac{4}{\pi} \times \mu_j$. Table 3 shows the final refinement of the components for the magnetic moment along the crystallographic directions of the primitive unit cell (a, b, c) in the antiphase structure, obtained from G61 at 1.5 K and those reported on D1B at 1.89 K. The magnetic model is based on the high-temperature FI arrangement ↑↓↑ adopting an antiphase ordering following the sequence +-+-, where + (-) means ↑↓↑ ↑↓↑ ↑↓↑ ↑↓↑ (↓↑↓ ↓↑↓ ↓↑↓ ↓↑↓) (see Fig. 2 (b)). This complex magnetic behavior where the system undergoes two magnetic phase transitions must be interpreted mainly as a consequence of the particular competition of superexchange interactions in $ND_4Fe(DPO_4)_2$ through Fe-O-P-O-Fe. This issue will be investigated in future works.

4. Conclusions

In summary, the $ND_4Fe(DPO_4)_2$ shows two magnetic phase transitions. Below $T_C = 17.82$ K the magnetic moments of the two sublattices of Fe^{3+} ions are coupled antiparallel on the ac-plane of the crystal structure having a FI ordering. When the temperature decreases below $T_t = 3.52$ K, the magnetic arrangement evolves to an antiphase one maintaining the same FI magnetic unit.

Acknowledgments
Financial support has been received from Spanish MEC and FEDER Grant No. MAT2008-06542-C04.

References
[1] Maspoch D, Ruiz-Molina D and Veciana J 2007 *Chem. Soc. Rev.* **36** 770
[2] Murugavel R, Choudhury A, Walawalkar M G, Pothiraja R and Rao C N R 2008 *Chem. Rev.* **108** 3549
[3] Mahata P, Sarma D, and Natarajan S 2010 *J. Chem. Sci.* **122** 19
[4] Riou-Cavellec M, Riou D and Férey G 1999 *Inorg. Chim. Acta* **291** 317
[5] Natarajan S and Mandal S 2008 *Angew. Chem. Int.* **47** 4798
[6] Alfonso B F, Trobajo C, Piqué C, Fernández-Díaz M T, Rodríguez Fernández J, Salvadó M A, Pertierra P, García-Granda S, García J R and Blanco J A 2010 *Acta. Materialia* **58** 1741
[7] Alfonso B F, Blanco J A, Fernández-Díaz M T, Trobajo C, Khainakov S A, and García J R 2010 *Dalton Trans.* **39** 1791
[8] Alfonso B F, Piqué C, Trobajo C, García J R, Kampert E, Zeitler U, Rodríguez Fernández J, Fernández-Díaz M T and Blanco J A 2010 *Phys. Rev. B* **82** 144431
[9] Alfonso B F, Piqué C, Trobajo C, García J R, Rodríguez Fernández J, Fernández-Díaz M T and Blanco J A 2011 Acepted for publication *J. Phys. Conference Series*
[10] Rodríguez–Carvajal J 1993 *Physica B* **192** 55
[11] Chevalier B, Etourneau J, Hagenmuller P, Quezel S and Rossat-Mignod J. 1985 *J. Less Common Metals* **111** 161
[12] Arfken G, 1970 *Mathematical Methods for Physicists* (Academic Press, New York)
[13] Blanco J A, Fåk, B, Ressouche E, Grenier B, Rotter M, Schmitt D, Rodríguez-Velámazan J A, Campo J and Lejay P 2010 *Phys. Rev. B* **82** 054414